

Development of a Power/Control Module for Urban Intelligent Electric Vehicles

Jyh-Ching Juang and Yu-Chi Chen

Department of Electrical Engineering, National Cheng Kung University, Tainan, TAIWAN

E-mail: juang@mail.ncku.edu.tw

Abstract

The paper is devoted to developing some key technologies of urban intelligent electric vehicles (EVs). Due to the worldwide environment and energy problems, the research on electric vehicle flourishes in last few years. Especially in the complex urban scenarios, how to meet the needs of energy efficiency and safety simultaneously becomes the primary issue of designing an urban EV. In this paper, the power/control module which adopts the control techniques is developed to fulfil these requirements of urban EVs. Besides, the power/control module is designed, implemented, integrated to the light-weight electric vehicle (LEV) platform, and tested to verify the functions and assess the performance.

Keywords: intelligent light-weight vehicle, intelligent control, electric car, wireless charging

1 Introduction

The intelligent transportation system (ITS) has become a hot issue in recent years [2][3], especially the applications in the complex urban environments. In these topics, due to the environment and energy concerns, the electric vehicle has attracted lots of attention. The trends in electric vehicle design aim to achieve the goals of better energy efficiency, environmental friendliness, convenience, and safety. Indeed, future urban transportation vehicles are likely to integrate electric-driven, green and clean, satellite navigation, communication, and intelligent techniques while employing electric or hybrid electric means for propulsion.

In order to fulfill the aforementioned requirements, the demanding tasks of an electric vehicle are the power management and intelligent control techniques. In the paper, the design and test of a power/control module for electric vehicles are discussed. The module of the electric vehicle facilitates efficient power

management, intelligent control, and coordinated guidance functions. This research dedicates to develop key technologies for the eventual realization of intelligent light-weight electrical vehicles as well as the associated transportation environment.

The paper is organized as following: section 2 depicts the overall LEV platform architecture. The section 3 describes the methodologies which are used in the power/control module, and the experiments and results of the module are provided in the section 4. Finally, the section 5 concludes the whole paper.

2 System Design

The system block diagram of the vehicle is depicted in Figure 1. To meet the requirements of the next-generation electric vehicle, the power/control module is composed of three main subsystems: the high-efficient power management subsystem, the heterogeneous sensor fusion based autonomous navigation subsystem, and the intelligent control subsystem.

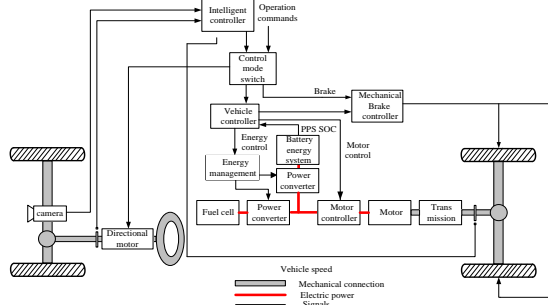


Figure 1 System Block Diagram

2.1 High-Efficient Power Management Subsystem

Since the next-generation EVs contain different energy sources and have to provide the power for various purposes, a high-efficient power management system is indispensable for the EVs. In this paper, the high-efficient power management subsystem is composed of an LiFe battery, a fuel cell and a high-quality DC/DC converter. Xiangjun Li et al [4] designed the vehicular power system model by using MATLAB and controlled the constructed dynamic model of the hybrid system by using fuzzy control techniques, and these power management techniques were tested through the simulations and the hybrid electric vehicle. Originating from this idea, in this subsystem, we use a fuel cell as the main power source and adopt an LiFe battery as the auxiliary power source to counterbalance the characteristics of the fuel cell such as slow dynamic response and sensitive to the variance of the load. In this subsystem, we also proposed a novel interleaved buck-boost converter which can be used as output regulation of fuel cell and energy transfer applications.

2.2 Autonomous Navigation Subsystem

The autonomous navigation subsystem is based on the heterogeneous sensor fusion techniques. The heterogeneous sensor fusion based autonomous navigation subsystem contains collision warning and path-planning techniques. The collision warning strategy is developed through a collision risk indicator (CRI) that can caution the driver for preventing potential accidents or aid the auto-driving function, which is a part of intelligent control subsystem, to improve the safety of vehicle and pedestrians.

2.3 Intelligent Control Subsystem

The intelligent control subsystem utilizes the navigation technique and the fuzzy controller to construct the function of auto-driving which can keep the LEV move on the lane. The auto-driving function exploits the properties of the optic sensor (camera) and the information of GPS.

3 Proposed Methodologies

In this paper, the new interleaved converter, collision avoidance system, path planning strategy and auto-driving technique are proposed and verified on the LEV platform. This section depicts these proposed techniques and describes how we integrate them on the LEV platform.

3.1 Proposed Interleaved Buck-Boost Converter

In the high-efficiency power management subsystem, we use a proposed interleaved buck-boost converter, as shown in Figure 2 which is used as the output regulation of fuel cell and the way of energy delivery between different power sources.

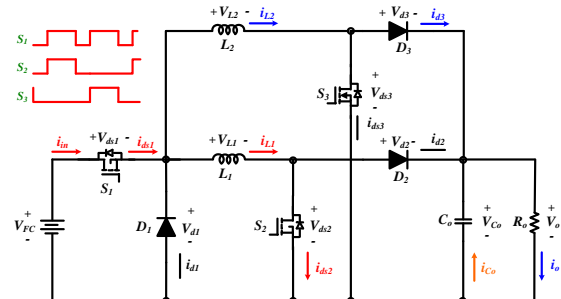


Figure 2 Proposed Interleaved Buck-Boost Converter

There are four modes of the waveforms (mode I through mode IV) in a cycle. Given that mode I and mode II are equivalent to mode III and mode IV respectively, one can only analyze the first two modes. In the mode I ($t_0 \sim t_1$), which has the equivalent circuit shown in Figure 3, the S_1 and S_2 are the turn-on state while S_3 is the cutoff state. Inductance L_1 is charged by input current through switch S_1 and S_2 , while input current and inductance L_2 provide energy to the output load through switch S_1 and diode D_3 .

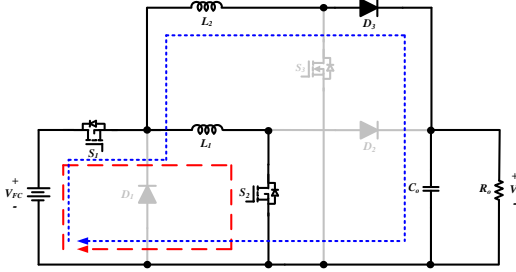


Figure 3 Equivalent Circuit of Mode I

In the mode II ($t_1 \sim t_2$), which has the equivalent circuit shown in Figure 4, switch S_1 , S_2 and S_3 are all in the cutoff state. Thus, inductance L_1 provides its energy to the output load through diode D_1 and D_2 , while inductance L_2 provides its energy through diode D_1 and D_3 .

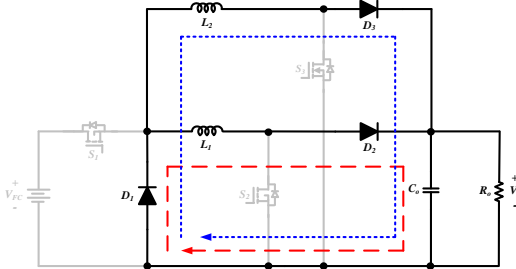


Figure 4 Equivalent Circuit of Mode II

The voltage gain of the proposed interleaved buck-boost converter is about two times higher than conventional buck-boost converters. Besides, the interleaved frame used in the proposed topology converter can eliminate the output current ripples.

3.2 Collision Warning System

In the autonomous navigation subsystem, a collision warning strategy with collision risk indicator (CRI) is established to aid the drivers and the auto-driving function in the intelligent control subsystem. In this paper, we adopt the GPS module and wireless communication techniques to overcome some difficulties in complex urban crossroad situations. The sensors used in the sensor fusion based collision warning strategy are GPS, Zigbee wireless modules and the Laser modules. The controller computes the CRI by using the information from these sensors. Once the CRI is greater than a threshold [1], the controller will send a warning signal to decelerate and stop the vehicle or change the lane of the vehicle.

The collision warning system utilizes the GPS receiver to get the position and direction of the vehicle, and the information of current speed comes from the encoder which is equipped at the motor of the rear wheels. Then the wireless communication modules transmit information of current vehicle, say vehicle B in Figure 7, including position, velocity, heading direction and time and simultaneously receive other vehicular information in the communication range. After receiving a vehicle's information, say vehicle A in Figure 5, the relative velocity vector $V(v, \theta_B)$, relative angle θ_A and relative distance d can be computed as shown in Figure 7.

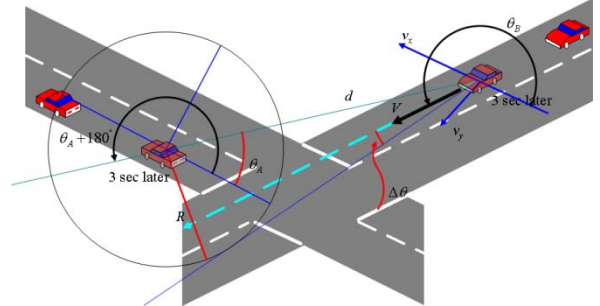


Figure 5 Collision Avoidance Strategy

Meanwhile, the collision warning system will estimate the position which the vehicle will be after k seconds. If estimated position of vehicle B after k seconds is in the circle which uses the position of vehicle A after k seconds as origin and R as radius, the collision warning system will calculate the collision risk indicator (CRI)[1] between two positions of two vehicles. The CRI can be defined as:

$$CRI = 10 \times \log \frac{10^5}{r_b \times t_c} \quad (1)$$

where r_b is the extended velocity vector of vehicle B, and t_c is the collision time which can be defined as:

$$t_c = \frac{d}{v} \quad (2)$$

where v is the relative velocity between two vehicles:

$$v = |\vec{v}_A - \vec{v}_B| \quad (3)$$

Once the CRI is higher than the threshold, the collision warning system will decelerate or stop the vehicle.

3.3 Path Planning Strategy

In our path planning strategy, we adopt the dendrogram to find the shortest path. We label

each intersection as n_i and store them in a matrix form. In order to reduce the computational complexity and the time of path planning, the comparison method used is the piece-wise continue comparison. The overall strategy of finding the shortest path is as follows:

Step 1. Label and number all intersections.

Step 2. Construct the relativity matrix \mathbf{N} .

Step 3. Start from the initial intersection and find its linked intersections. The distances between the linked intersections will be accumulated. Based on the latitude and longitude, when the differences between the accumulated distances of the two intersections is smaller than a threshold, the accumulated distances will be compared and save the shorter path.

Step 4. Repeat Step 3 until the final intersection is reached.

3.4 Auto-Driving Techniques

The core of the intelligent control subsystem is the auto-driving techniques, which includes the sensor fusion, lane detection and following and vehicle velocity control.

The block diagram of the sensor fusion system is shown in the Figure 12. This system integrates the information from GPS, and optic sensor (camera) as well as the electronic compass and the inertial measurement units (IMU, which includes three-axis accelerometer, magnetometer and gyroscope) to make the vehicle move as planned. The system utilizes the camera to detect lane and compute the control commands for vehicle through captured images [5][6].

As to the position estimation, GPS provides information of latitude and longitude to calibrate the position which is estimated by integral computations. As to the velocity estimation, it uses GPS information to compensate the velocity sensor because the variations in the latitude and longitude can be used to estimate the velocity as well. As to the inclination of the vehicle, the system uses inclination angles measured by IMU as the reference of angles estimated by the gyro sensor. It can efficiently eliminate the accumulated measurement error produced by sensor drift through the use of Kalman filter to compute the sensor information. The azimuth angle estimation mainly bases on the magneto-sensor or the electronic compass. When moving in the real world scenarios, the vehicle will encounter uphill and downhill; in these situations, the estimation error made by magneto-sensor will

increase, so the electronic compass needs inclination compensation. However, the facilities such as the engine on the vehicle will interfere with the electronic compass. Thus, GPS information will compensate the estimation of the azimuth angle. The azimuth angle of the vehicle can be obtained by GPS using (4).

$$\theta = \tan^{-1} \left(\frac{\sin(\lambda_B - \lambda_A) \cos \phi_B}{\cos \phi_A \sin \phi_B - \sin \phi_A \cos \phi_B \cos(\lambda_B - \lambda_A)} \right) \quad (4)$$

where λ_A , λ_B , ϕ_A and ϕ_B are the longitude and the latitude of position A and position B respectively. The azimuth angle θ obtained from (4) is the angle between the vehicular direction and the grid north. If the vehicle is heading west, the azimuth angle θ is equal to zero. Position A is the previous longitude and latitude GPS measured while position B is the current longitude and latitude GPS measured. Once the vehicle stops, which means position A is equal to position B, the equation (5) cannot be used to calculate the azimuth angle; thus, the information of azimuth angle mainly comes from the electronic compass.

The lane detection is the main issue in the auto-driving function. We use the camera to capture the images and output the control commands to the vehicle. The algorithm used in the lane detection is originated from [6]. Shadows have serious impacts on lane detections. Reference [6] utilizes the gray scale images, which can be transformed from RGB images by using equation (5), to lessen the influence of shadows while improving the capability of identifications. The transformation from RGB to gray scale images can be written as:

$$I_1 = \log \frac{R}{G} \cos \beta + \log \frac{B}{G} \sin \beta \quad (5)$$

where I_1 represents the gray value of the gray scale images, R, G, B are the value of the RGB images and the β is the camera-related parameters which can be obtained from calibration of the camera. In order to boost the identification efficiency and alleviate the impact of shadows in the lane detection, we propose another transformation function to achieve the requirements, as shown in (6):

$$I_2 = \log \frac{R}{B} \cos \alpha + \log \frac{G}{B} \sin \alpha \quad (6)$$

where I_2 represents the gray value of the gray scale images, and α is the camera-related parameters which can also be obtained from the camera calibration. However, α and β can be calibrated independently and will not affect each

other. We use both equations to transform the same RGB image into two gray scale images and identify the lane only when the regions in both gray scale images are detected as lane. Once the lane is detected, one can control the steering-wheel to navigate the vehicle. The methodology we use in this paper is that the trapezoid mask is adopted into the detected lane region.

This paper uses the line between the gravity center of the trapezoid mask and the centered point of the bottom line as the heading direction of the vehicle. The gravity center of the trapezoid can be calculated by

$$C_x = \frac{\sum D_{ix} V_i}{\sum V_i}, C_y = \frac{\sum D_{iy} V_i}{\sum V_i} \quad (7)$$

where the C_x and C_y are the coordinates of the gravity center of the trapezoid mask, i addresses the index, the D_{ix} and D_{iy} are the coordinates of the four vertexes of the trapezoid mask and the V_i is the gray value of the vertex i .

When the vehicle needs to turn left or right, the GPS and the electric compass can come into play. By applying equation (4), one can obtain the heading direction of the vehicle. Based on these sensor fusion techniques, the vehicle can identify the lane and the obstacles in the environment. Combined with the autonomous control system, the vehicle can reach the goal of autonomous navigation. By adopting the sensor fusion system, the block diagram of the auto-driving function can be constructed, as shown in Figure 6.

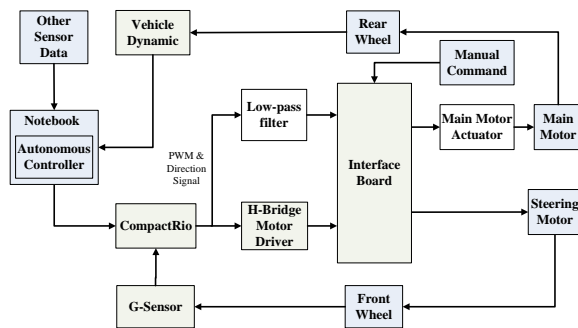


Figure 6 Auto-Driving System Block Diagram

4 Experiments and Results

4.1 High-Efficiency Power Supply Subsystem Experiments

The converter circuit of the proposed interleaved buck-boost converter is shown in Figure 7, and the efficiency of the proposed converter is shown in Figure 8. The red-dotted line in Figure 8 represents the circuit input voltage, which is the output voltage of the fuel cell, decreases when the load increases. As shown in Figure 8, the characteristic of the fuel cell make its output voltage 39.6 volt drop to 29.1 volt when it is fully loaded. The blue-dotted line is the efficiency curve, which shows that the highest efficiency of the circuit can reach 90.3% while it still maintain the efficiency at 85.7% when it is full-loaded.

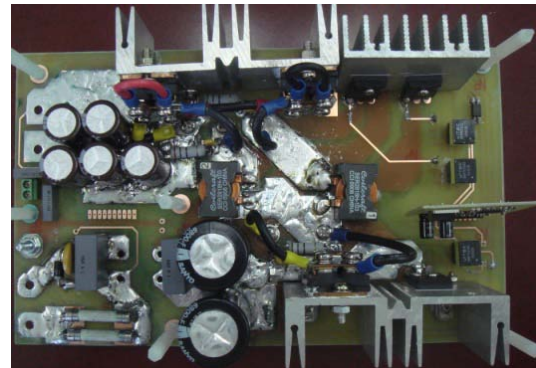


Figure 7 Converter Circuit

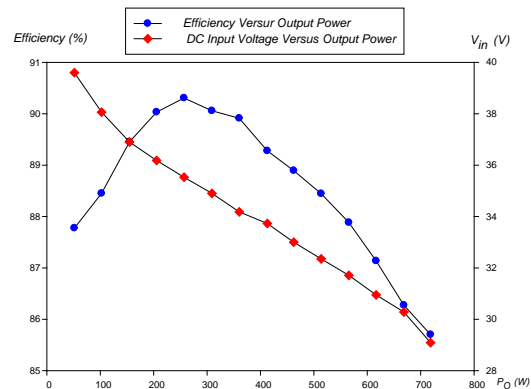


Figure 8 Converter Efficiency

Furthermore, we construct a hybrid power supply system, which is a part of the high-efficiency power management subsystem, of our LEV platform with this proposed converter. The input voltage of the proposed converter ranges from 26 to 45 volts and then the converter stably

outputs 24 volts to the DC bus. (The LiFe battery also outputs its energy to DC bus.)

4.2 Autonomous Navigation Subsystem Experiments

In this subsystem experiment, we verify two proposed strategies which are the shortest path finding and the collision warning system.

In the shortest path finding experiment, the simulated traffic network used in the experiment is shown in Figure 9.



Figure 9 Simulated Traffic Network

In the experiment of collision warning system, the collision warning system, which integrates GPS (vehicular location positioning), ZigBee (vehicular information receiving) and CompactRIO (CRI computing), is shown in Figure 10. After GPS locates the vehicle and ZigBee module receives the vehicular information from itself and other vehicles, these information will transmit to CompactRIO through RS232 interface. After receiving the information from each vehicle, CompactRIO will calculate the relative distance, angle and heading directions between two vehicles. Once these values are computed, the CompactRIO can compute the relative velocity between two vehicles and the extended velocity vector r_b and the collision time t_c in (1). The interface of the collision warning system is depicted in Figure 11.

4.3 Intelligent Control Subsystem Experiments

In the intelligent control subsystem, the proposed methods which need to be verified are the lane detection and the auto-driving function.

Figure 12 shows the user interface of lane detection which is programmed by the LabView. The leftmost image is transformed from the captured RGB image through equation (5) while the middle image is transformed through equation (6). The result of the lane detection is shown in the rightmost image and the computation time is about 0.2 second which can be less than 0.2 second if the images need not to be shown in user interface.

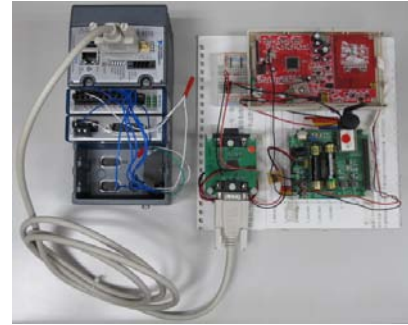


Figure 10 Collision Warning System

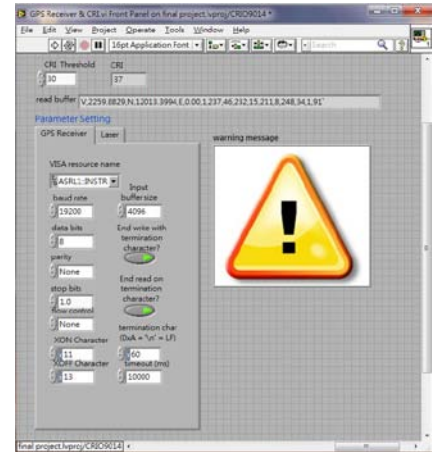


Figure 11 GUI of Collision Warning System

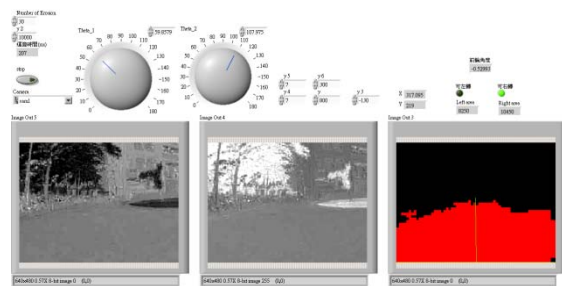


Figure 12 LabView Interface of Lane Detection

Figure 13 shows the user interface of the auto-driving function. This panel displays the received information from the GPS module, the electric compass, the gravity sensor and the results of lane detection. Also, if the system detects the vehicle

should turn left or right, the system will determine the direction of the vehicle through the captured images and the GPS information. Once the system determines the vehicle should turn right or left, the LED on the left of the user interface will turn on.

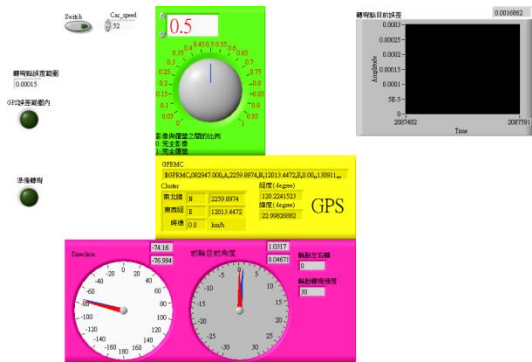


Figure 13 LabView Interface of Auto-Driving Function

The experimental path of the auto-driving function is shown in Figure 26. In the experiments, by adopting these sensor fusion control techniques, the LEV platform moved as planned smoothly both in the straight road and the turning sections.

5 Conclusions

In this paper, an LEV platform has established and equipped the high-efficiency power management subsystem, the autonomous navigation subsystem and the intelligent control subsystem. Besides, in this paper, we propose several techniques in the power/control modules which are also verified by the on-road experiments through the LEV platform. The proposed DC/DC interleaved buck-boost converter has been integrated into the hybrid power supply system and it has been verified through experiments of load variances. Also, the shortest path finding strategy and the collision warning system are designed and verified through on-road experiments. Finally, the proposed auto-driving techniques which includes the lane detection and sensor fusion techniques are established and tested through simulations and on-road tests.

Acknowledgments

The work was supported by the National Science Council, Taiwan under grant NSC 99-2218-E-006-006.

References

- [1] Ueki, S. Tasaka, Y. Hatta, and H. Okada, "Vehicular-Collision Avoidance Support System (VCASS) by Inter-Vehicle Communications for Advanced ITS," *IEICE Transactions on Fundamentals of Electronics, Communications and Computer Sciences*, Vol. E88-A, No. 7, pp. 1816-1823, 2005.
- [2] A. W. Krings and P. R. Merry, "A functionality based hierarchical model for survivable intelligent transportation systems," *IEEE Intelligent Transportation Systems Magazine*, pp. 20-26, Apr. 2009.
- [3] J. Yi and R. Horowitz, "Macroscopic Traffic Flow Stability for Adaptive Cruise Controlled (ACC) Vehicle," *Proceedings of the 41st IEEE Conference on Decision and Control*, pp. 893-899, Dec. 2004.
- [4] X. Li, L. Xu, J. Hua, X. Lin, J. Li, M. Ouyang, "Power management strategy for vehicular-applied hybrid fuel cell/battery power system", *Journal of Power Sources*, Vol.191, no.2, pp. 542-549, Jun. 2009.
- [5] A. El Hajjaji, S. Bentalba, "Fuzzy path tracking control for automatic steering of vehicles", *Robotics and Autonomous Systems*, vol.43, pp. 203–213, 2003.
- [6] J.M.A. Alvarez and A.M. López, "Road Detection Based on Illuminant Invariance," *IEEE Transactions on Intelligent Transportation Systems*, VOL. 12, NO. 1, pp. 184-193, 2011

Authors

Jyh-Ching Juang received the B. S. and M. S. degrees from National Chiao-Tung University, Hsin-Chu, Taiwan, in 1980 and 1982, respectively, and the Ph. D. degree in electrical engineering from University of Southern California, Los Angeles, in 1987. He was with Lockheed Aeronautical System Company, Burbank before he joined the faculty of the Department of Electrical Engineering, National Cheng Kung University, Tainan, Taiwan in 1993. His research interests include sensor networks, GNSS signal processing, and software-based receivers

